**Article:**
Li, K. C.W., Neveling, R., Adsley, P. et al. (14 more authors) (2017) Characterization of the proposed 4-α cluster state candidate in O 16. Physical Review C. 031302. ISSN 2469-9993

https://doi.org/10.1103/PhysRevC.95.031302

PHYSICAL REVIEW C **95**, 031302(R) (2017)

# Characterization of the proposed 4-$\alpha$ cluster state candidate in $^{16}$O

K. C. W. Li,[1,2,*] R. Neveling,[2] P. Adsley,[1,2] P. Papka,[1,2] F. D. Smit,[2] J. W. Brümmer,[1] C. Aa. Diget,[3] M. Freer,[4] M. N. Harakeh,[5] Tz. Kokalova,[4] F. Nemulodi,[2] L. Pellegri,[2,6] B. Rebeiro,[7] J. A. Swartz,[8,†] S. Triambak,[7] J. J. van Zyl,[1] and C. Wheldon[4]

[1]*Department of Physics, University of Stellenbosch, Private Bag X1, 7602 Matieland, South Africa*
[2]*iThemba LABS, National Research Foundation, P.O. Box 722, Somerset West 7129, South Africa*
[3]*Department of Physics, University of York, Heslington, York YO10 5DD, United Kingdom*
[4]*School of Physics and Astronomy, University of Birmingham, Edgbaston, Birmingham B15 2TT, United Kingdom*
[5]*University of Groningen, KVI Center for Advanced Radiation Technology, 9700 AB Groningen, The Netherlands*
[6]*School of Physics, University of the Witwatersrand, Johannesburg 2050, South Africa*
[7]*Department of Physics, University of the Western Cape, Private Bag X17, Bellville ZA-7535, South Africa*
[8]*KU Leuven, Instituut voor Kern- en Stralingsfysica, Celestijnenlaan 200D, B-3001 Leuven, Belgium*

(Received 27 October 2016; published 3 March 2017)

The $^{16}$O($\alpha$,$\alpha'$) reaction was studied at $\theta_{\rm lab} = 0^\circ$ at an incident energy of $E_{\rm lab} = 200$ MeV using the K600 magnetic spectrometer at iThemba LABS. Proton decay and $\alpha$ decay from the natural parity states were observed in a large-acceptance silicon strip detector array at backward angles. The coincident charged-particle measurements were used to characterize the decay channels of the $0^+_6$ state in $^{16}$O located at $E_x = 15.097(5)$ MeV. This state is identified by several theoretical cluster calculations to be a good candidate for the 4-$\alpha$ cluster state. The results of this work suggest the presence of a previously unidentified resonance at $E_x \approx 15$ MeV that does not exhibit a $0^+$ character. This unresolved resonance may have contaminated previous observations of the $0^+_6$ state.

DOI: 10.1103/PhysRevC.95.031302

Light nuclei are expected to exhibit clusterlike properties in excited states with a low-density structure. Such states should exist particularly at excitation energies near the separation energies for these clusters, as described by the diagram of Ikeda *et al.* [1]. The Hoyle state, the $0^+_2$ state at $E_x = 7.654$ MeV in $^{12}$C, is considered the archetype of a state that exhibits $\alpha$-particle structure, with one option being a 3-$\alpha$ gaslike structure similar to a Bose-Einstein condensate consisting of three $\alpha$ particles all occupying the lowest $0S$ state [2]. It is expected that equivalent Hoyle-like states should also exist in heavier $\alpha$-conjugate nuclei such as $^{16}$O and $^{20}$Ne [3]. Early discussions of extended structures in $^{16}$O were instigated by the seminal work of Chevallier *et al.* [4] who investigated low-energy $\alpha + {}^{12}$C scattering. The search for analogues of the Hoyle state in heavier $\alpha$-conjugate nuclei is ongoing. Candidate states in $^{16}$O below the four-$\alpha$-particle breakup threshold ($S_{4\alpha} = 14.437$ MeV) include the $0^+_4$ state at $E_x = 13.6(1)$ MeV, discovered in 2007, observed via inelastic scattering at $E_{\rm lab} = 400$ MeV [5]. Another candidate is the $0^+_5$ state at $E_x = 14.032(15)$ MeV [6], known to be strongly excited via monopole transitions from the ground state. A potential Hoyle-like candidate above the four-$\alpha$-particle breakup threshold in $^{16}$O has been identified by Funaki *et al.* [7], who solved a four-body equation of motion based on the orthogonality condition model that succeeded in reproducing the observed $0^+$ spectrum in $^{16}$O up to the $0^+_6$ state. It was suggested that the 4-$\alpha$ condensation state could be assigned to the $0^+_6$ state at $E_x = 15.097(5)$ MeV [8] (see Table I). The $0^+_6$ state obtained from the calculation is 2 MeV above the four-$\alpha$-particle breakup threshold and has a large radius of 5 fm, indicating a dilute density structure. Ohkubo and Hirabayashi showed in a study of $\alpha + {}^{12}$C elastic and inelastic scattering [9] that the moment of inertia of the $0^+_6$ state is drastically reduced, which suggests that it is a good candidate for the 4-$\alpha$ cluster condensate state. Calculations performed with the Tohsaki-Horiuchi-Schuck-Röpke (THSR) $\alpha$-cluster wave function [10] also support this notion with an estimated total width of 34 keV for the $0^+_6$ state [11], much smaller than the experimentally determined value of 166(30) keV [12].

Recent unsuccessful attempts to measure particle decay widths of the $0^+_6$ state in $^{16}$O [17,18] highlighted the need for an experiment that combines $\alpha$-particle decay measurements with a high-energy-resolution experimental setup and a reaction capable of preferentially populating $0^+$ states. In contrast to transfer reaction measurements, inelastic $\alpha$-particle scattering at zero degrees has the advantage that it predominantly excites low-spin natural parity states. A measurement of the $^{16}$O($\alpha$,$\alpha'$) reaction at zero degrees, coupled with coincident observations of the $^{16}$O decay products, was performed at the iThemba Laboratory for Accelerator-Based Sciences (iThemba LABS)

TABLE I. Literature values for the $0^+_6$ state in $^{16}$O.

| Reference | Year | $E_R$ (MeV) | Width (keV) | Reaction |
|---|---|---|---|---|
| [13] | 1972 | 15.17(5) | 190(30) | $^{12}$C($\alpha$,$\alpha'$) |
| [14] | 1978 | 15.10(5) | 327(100) | $^{15}$N($p$,$\alpha$),$^{15}$N($p$,$p'$) |
| [15] | 1978 | 15.103(5) | – | $^{14}$N($^3$He,$p$) |
| [16] | 1982 | 15.066(11) | 166(30) | $^{12}$C($\alpha$,$\alpha'$),$^{15}$N($p$,$\alpha$) |
| [8] | 2016 | 15.097(5) | 166(30) | – |
| This work | 2016 | 15.076(7) | 162(4) | $^{16}$O($\alpha$,$\alpha'$) |

*kcwli@sun.ac.za
†Present address: Department of Physics and Astronomy, University of Aarhus, DK-8000 Aarhus C, Denmark.

 

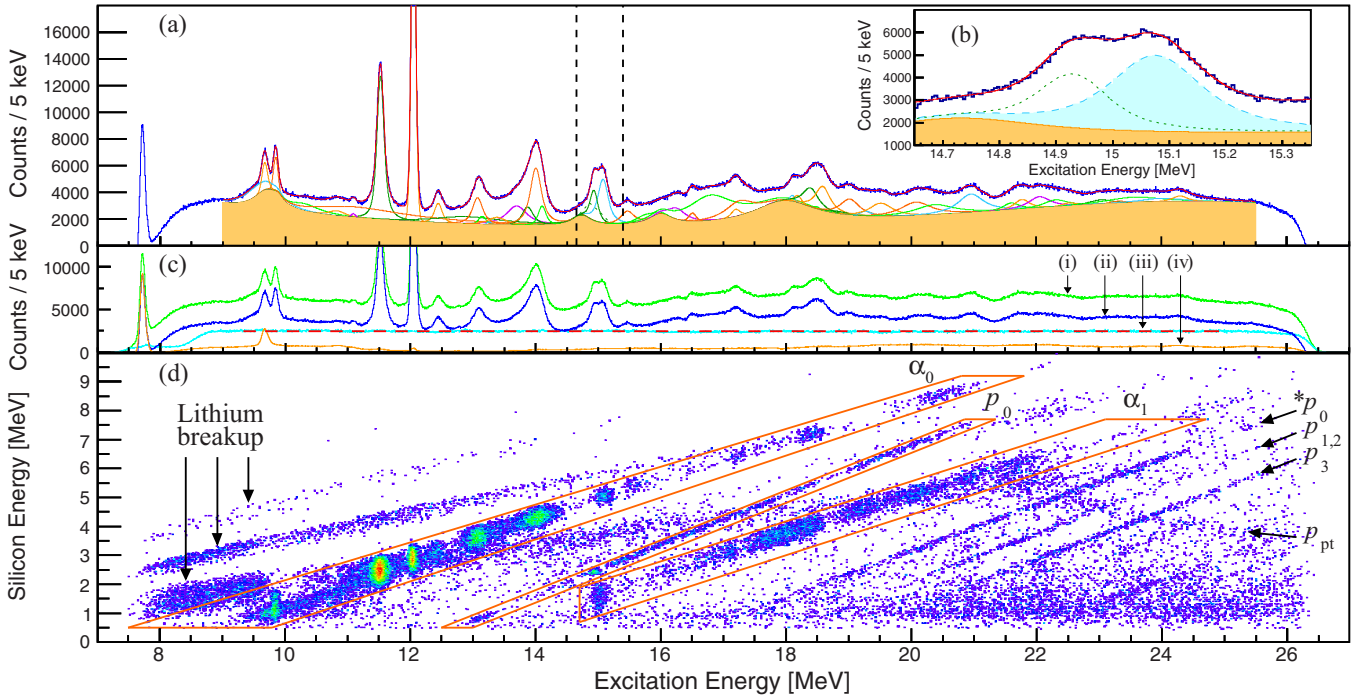


FIG. 1. (a) The background-subtracted inclusive excitation spectrum from the $Li_2CO_3$ target, with fitted $R$-matrix Voigt line shapes that are superimposed upon the background of fitted lithium resonances (filled in orange). (b) The excitation energy region of interest highlighting the $0^+_6$ resonance (dashed blue line) and the neighboring $J^\pi = 2^+$ resonance (dotted green line). (c) The raw (i), background-subtracted (ii), and instrumental background inclusive excitation (iii) spectra from the $Li_2CO_3$ target. Spectrum (iv) is the background-subtracted inclusive excitation spectrum from the $^{12}C$ target, normalized to spectrum (ii) through the 9.641(5) MeV resonance in $^{12}C$. The linear fit of spectrum (iii), used for background subtraction, is displayed as a dashed red line. (d) The coincident matrix of silicon energy versus the excitation energy of the recoil nucleus for decay particles detected within the angular range: $156^\circ < \theta_{lab} < 163^\circ$ (two silicon strips within the array). The $\alpha_0$-, $\alpha_1$-, and $p_{0-3}$-decay lines from $^{16}O$ are indicated. The proton punch-through structure from the $p_0$ decay is labeled $p_{pt}$. The lithium breakup and the $^*p_0$-decay line from $^{12}C$ are indicated. A display color threshold of >1 is imposed.

in South Africa. A 200-MeV dispersion-matched $\alpha$-particle beam was provided by the separated sector cyclotron. The $\alpha$ particles that were inelastically scattered off a $^{nat}Li_2CO_3$ target were momentum analyzed at zero degrees with the K600 magnetic spectrometer [19]. The energy resolution obtained was 85(1) keV full width at half maximum (FWHM), determined from the 12.049(9) MeV resonance in $^{16}O$. The error on the calculated excitation energy was $\delta E_x < 9$ keV. The 510-$\mu$g/cm$^2$-thick $^{nat}Li_2CO_3$ target was prepared on a 50-$\mu$g/cm$^2$-thick $^{12}C$ backing. The total $^{nat}Li$ content was approximately 50 $\mu$g/cm$^2$ [20]. The solid-angle acceptance of the spectrometer (3.83 msr) was defined by a circular collimator with an opening angle $\pm 2^\circ$. A comprehensive description of the experimental and analysis techniques is reported elsewhere [21].

The inclusive excitation energy spectra are displayed in Figs. 1(a), 1(b), and 1(c). To extract the excitation energy spectrum for the $^{16}O(\alpha,\alpha')$ reaction, the instrumental background must be taken into account and the contributions from the carbon and lithium present in the target must be identified. The flat and featureless instrumental background, indicated as spectrum (iii) in Fig. 1(c), is typical for measurements at zero degrees. It results from small-angle elastic scattering off the target foil that is followed by rescattering off any exposed part inside the spectrometer [19]. To subtract this background contribution, the spectrometer was operated in focus mode where the quadrupole at the entrance to the spectrometer was used to vertically focus reaction products to a narrow horizontal band on the focal plane. The background spectrum was generated by using the sections of the focal plane above and below the vertically focused band. A linear fit was employed to approximate the background and was subtracted from the raw spectrum (i) to produce spectrum (ii). The background-subtracted focal plane spectrum from the $^{12}C$ target (iv) was normalized to spectrum (ii) through the 9.641(5)-MeV resonance in $^{12}C$. The smooth contribution observed from $^{12}C$ in the excitation energy region of interest ($E_x \approx 15$ MeV) combined with the broad resonances of $^7Li$ and $^6Li$ indicated by the orange band in Figs. 1(a) and 1(b) ensure that the distinctly observed resonances can be assigned to $^{16}O$. At $E_x \approx 15$ MeV, the decay modes from $^{16}O$ are not affected by the lithium breakup indicated in Fig. 1(d).

The decay products were observed with the Coincidence Array for K600 Experiments (CAKE) [22], consisting of four TIARA HYBALL MMM-400 double-sided silicon strip detectors (DSSSDs). Each of the 400-$\mu$m-thick wedge-shaped DSSSDs consisted of 16 rings and 8 sectors and were positioned at backward angles with the rings covering the polar-angle range of $114^\circ < \theta_{lab} < 166^\circ$, resulting in a solid-angle coverage of 20.4(5)% of $4\pi$. For each focal-plane event,

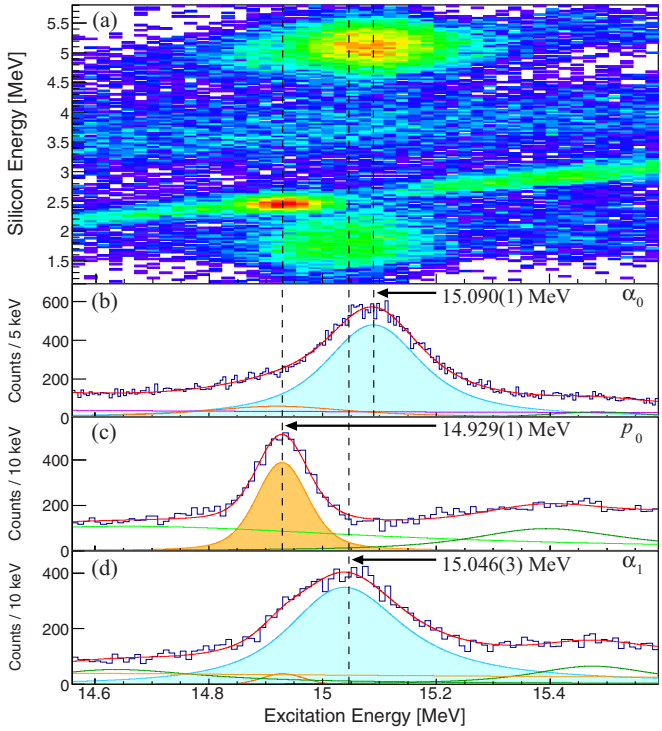


FIG. 2. (a) The coincident matrix of silicon energy versus the excitation energy of the recoil nucleus, highlighting the decay modes observed at the excitation energy region of interest at $E_x \approx 15.1$ MeV. The excitation energy projections of the $\alpha_0$-, $p_0$-, and $\alpha_1$-decay lines are displayed in panels (b), (c), and (d), respectively. The resonance energies, extracted with single-channel $R$-matrix fits, are indicated.

all signals from CAKE within a time window of 6 $\mu$s were digitized, yielding both K600 inclusive as well as K600 + CAKE coincidence events. A beam pulse selector at the entrance of the cyclotron (which accepted one in five pulses) was employed to ensure a sufficient time window (273 ns) for coincidence measurements.

The detection of coincident charged-particle decay with the CAKE array enables the characterization of resonances through the measurement of branching ratios and angular correlations of various decay modes. The associated decay lines of the $^{16}$O nucleus are displayed in Fig. 1(d): $\alpha$ decay and proton decay to the ground state of the residual nucleus are designated $\alpha_0$ and $p_0$, respectively, while $\alpha$ decay to the first excited state is designated $\alpha_1$. By gating upon a particular decay line and projecting onto excitation energy, the resonance line shape corresponding to a particular decay mode can be observed in isolation. The excitation energy spectra around $E_x \approx 15$ MeV corresponding to the $\alpha_0$-, $p_0$-, and $\alpha_1$-decay modes are displayed in Figs. 2(b), 2(c), and 2(d), respectively. The extensive decay data for other resonances shall be published in a more comprehensive paper.

Resonances in the energy range of interest exhibit an $R$-matrix Lorentzian line shape:

$$N(E) \propto \frac{\Gamma(E)}{[E - E_R]^2 + [\Gamma(E)/2]^2}, \tag{1}$$

where $E_R$ is the resonance energy (location parameter) and the total width, $\Gamma(E)$, is a sum of the energy-dependent partial widths. For the $i$th decay channel, the partial width is given by

$$\Gamma_i(E) = 2\gamma_i^2 P_l(E), \tag{2}$$

where $\gamma_i$ is the reduced width and $P_l(E)$ is the associated penetrability, corresponding to the orbital angular momentum of decay $l$ and the chosen external radius given by $R = 1.2 \times (A_1^{1/3} + A_2^{1/3})$. Given the inherent resolution of the focal plane detector system, the experimentally observed line shape of a resonance takes the form of a convolution between a Gaussian and the aforementioned $R$-matrix Lorentzian line shape, approximated by a Voigt line shape [23] with an $R$-matrix energy-dependent width, $\Gamma(E)$.

A single-channel $R$-matrix fit was implemented across the entire range of the focal plane considering possible resonances from all four target nuclei: $^{16}$O, $^{12}$C, $^{7}$Li, and $^{6}$Li. The Voigt line shapes within the fit were assigned the experimental energy resolution of FWHM = 85(1) keV. For all fitted resonances, the decay parameters of each line shape were chosen to correspond to the decay channel with the lowest orbital angular momentum. For each resonance with unknown branching ratios, the line shape was prescribed the decay channel parameters corresponding to the most strongly observed decay mode of the resonance (from this work). The fitted resonance energy, $E_R$, of each known resonance was constrained to within $3\sigma$ about its literature value (excluding the resonances at $E_x \approx 15$ MeV). An upper limit on the width, known as the Wigner limit [24], was imposed on each decay channel. The extracted total width of each resonance, $\Gamma(E)$, is evaluated at the associated resonance energy $E_R$ [see Eq. (2)]. In the inclusive spectrum displayed in Figs. 1(a) and 1(b), a prominent resonance was observed at $E_x = 15.076(7)$ MeV with an associated width of 162(4) keV. This is in good agreement with previous measurements of the $0_6^+$ resonance, as displayed in Table I. In contrast, the observed width of 101(3) keV for the neighboring $J^\pi = 2^+$ resonance at $E_R = 14.926(2)$ MeV does not agree well with the corresponding literature value of 54(5) keV. By fitting the focal plane spectra gated on the $\alpha_0$-, $p_0$-, and $\alpha_1$-decay modes, the resonance energies and widths from the resonances at $E_x \approx 15$ MeV were extracted, as displayed in Table II.

By gating on events detected in particular rings in the CAKE array, angular correlations of decay can be extracted in the laboratory reference frame, as shown in Fig. 3. Self-consistency of the $R$-matrix fits for the angular correlations was achieved by fixing the resonance energies and widths to the values extracted from the total fit of the relevant decay mode. To calculate the theoretical angular correlations of decay in the laboratory frame, the differential cross sections for the population of natural parity states through the $^{16}$O($\alpha$,$\alpha'$) reaction were calculated in the distorted-wave Born approximation with the code CHUCK3 [25]. Both the $m$-state population ratios and the angular correlations of subsequent particle decay from the recoil nucleus were then calculated with ANGCOR [26] in the inertial reference frame of the recoil nucleus. Considering the $^{16}$O($\alpha$,$\alpha'$) reaction with an incident energy of $E_{\rm lab} = 200$ MeV and a recoil excitation energy of $E_x = 15.0$ MeV, the angular acceptance of the ejectile $\alpha$ particle corresponds

TABLE II. Extracted single-channel $R$-matrix fit parameters from the inclusive and coincidence spectra.

| $J^\pi$ | Decay mode | $E_R$ (MeV) | $\Gamma_{\text{total}}$ (keV) | Branching ratio (%) |
|---|---|---|---|---|
| $2^+$ | Inclusive | 11.520(9) | 80(1) | – |
| | $\alpha_0$ | 11.521(9) | 82(1) | 109(3) |
| $0^+$ | Inclusive | 12.049(9) | 5(1) | – |
| | $\alpha_0$ | 12.049(8) | 12(1) | 96(3)[a] |
| $2^+$ | Inclusive | 14.930(8) | 101(3) | – |
| | $p_0$ | 14.929(8) | 40(1) | 21(1) |
| $0^+$ | Inclusive | 15.076(7) | 162(4) | – |
| | $\alpha_0$ | 15.090(7) | 162(4) | 72(2)[b] |
| | $\alpha_1$ | 15.046(8) | 216(10) | 67(3)[b] |

[a]The $\alpha_1$-decay channel was not observable within this work due to electronic thresholds of the CAKE array.

[b]The $\alpha_0$ and $\alpha_1$ branching ratios are calculated under the assumption that they both originate from a single $J^\pi = 0^+$ resonance. The summed branching ratios far exceed 100%, indicating that this assumption is false.

to recoil nuclei ($^{16}$O) with minimum and maximum kinetic energies of 80 keV ($\theta_{\text{lab}} = 0^\circ$) and 140 keV ($\theta_{\text{lab}} = 40^\circ$), respectively. To account for the velocity of the recoil nuclei, the calculated correlations are then relativistically transformed to the laboratory frame by taking into account the angular acceptance for the ejectile nuclei by the spectrometer. The solid-angle correction factors for the CAKE array are obtained with a GEANT4 [27] simulation which accounts for a potential ±2 mm positioning error that has been propagated through to the total error of the data points. Calculated angular correlations are shown in Fig. 3.

The data suggest the presence of a previously unidentified resonance at $E_x \approx 15$ MeV. Fig. 3(e) shows that the angular distribution of $\alpha_0$ decay observed at $E_R = 15.090(7)$ MeV is distinctly anisotropic. This can only result from the presence of a previously unidentified resonance with nonzero spin, which may be obscuring the isotropic decay of the $J^\pi = 0^+_6$ resonance. The calculated angular correlations of $\alpha_0$ decay from $J^\pi = 0^+$, $1^-$, $2^+$, $3^-$, $4^+$, and $5^-$ resonances at this resonance energy do not fit well to the data. The two best-fitting $\alpha_0$ angular correlations correspond to a $J^\pi = 0^+$ and a $J^\pi = 1^-$ resonance, yielding $\chi^2_{\text{red}} = 13.54$ and $\chi^2_{\text{red}} = 16.65$, respectively. Given the possibility of two distinct but unresolved resonances, all possible pairs of the calculated correlations were incoherently summed and fitted to the data (with the relative contributions being free parameters). These calculations do not yield satisfactory reproduction of the data: the best fit corresponds to the incoherently summed $\alpha_0$-decay distributions from a $J^\pi = 1^-$ and a $J^\pi = 5^-$ resonance, yielding $\chi^2_{\text{red}} = 7.67$. It is possible that the angular correlations of these inherently overlapping resonances may interfere. The anisotropy remains a clear identifier of a resonance with nonzero spin. To ensure that the anisotropy is not a consequence of the analysis, the angular correlations of decay from the most prominently observed resonances are also analyzed. The $\alpha_0$ angular distribution of the $J^\pi = 0^+$ resonance at $E_x = 12.049(9)$ MeV, shown in Fig. 3(b), exhibits isotropy and the corresponding calculation fits the data with a reduced chi-squared of $\chi^2_{\text{red}} = 1.01$, indicating that the experimental setup is well understood. Similarly for the $\alpha_0$ angular distribution of the $J^\pi = 2^+$ resonance at $E_x = 11.520(9)$ MeV displayed in Fig. 3(a), the theoretical fit is reasonable and yields $\chi^2_{\text{red}} = 1.42$.

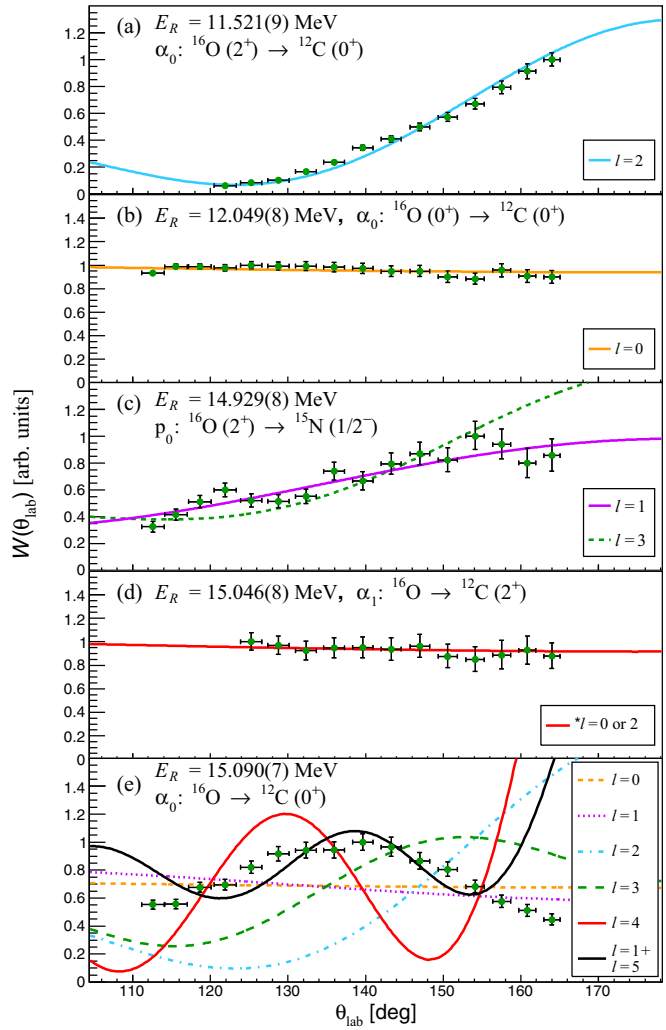


FIG. 3. Angular correlations of charged-particle decays from $^{16}$O in the laboratory frame relative to the beam axis: (a) $\alpha_0$ decay from the 11.521(9) MeV $J^\pi = 2^+$ resonance, (b) $\alpha_0$ decay from the 12.049(8) MeV $J^\pi = 0^+$ resonance, (c) $p_0$ decay from the 14.929(8) MeV $J^\pi = 2^+$ resonance, (d) $\alpha_1$ decay observed at 15.046(8) MeV, and (e) $\alpha_0$ decay observed at 15.090(7) MeV. *The $\alpha_0$ decays from $J^\pi = 0^+$ and $2^+$ resonances, corresponding to $l = 0\hbar$ and $2\hbar$, respectively, exhibit the same angular correlations. Data points affected by the electronic thresholds of the CAKE array are omitted.

The angular distribution of the $\alpha_1$-decay mode observed at $E_x = 15.046(8)$ MeV is observed to be isotropic, as displayed in Fig. 3(d). While only a $J^\pi = 0^+$or $2^+$ resonance can exhibit purely isotropic $\alpha_1$ decay, inherently anisotropic decays from resonances of other spin-parities may experimentally appear isotropic given their multiple possible $l$ values of decay. It is therefore assumed that this $\alpha_1$-decay mode originates from

the $J^\pi = 0_6^+$ resonance. The fit to the calculated $\alpha_1$ $J^\pi = 0^+$ angular distribution yields $\chi^2_{\rm red} = 0.15$, which could indicate either an overestimation of the data errors or that the dominant error is a systematic scaling factor. This, however, does not affect the conclusions of the paper. The angular distribution of the $p_0$-decay mode observed at $E_x = 14.929(8)$ MeV is displayed in Fig. 3(c). The proton decay from a $J^\pi = 2^+$ resonance to the $J^\pi = 1/2^-$ ground state of $^{15}$N corresponds to orbital angular momenta of decay of either $l = 1\hbar$ or $3\hbar$, corresponding to calculated correlations which fit with $\chi^2_{\rm red} = 1.25$ and 4.57, respectively.

Additional evidence towards a previously unidentified resonance is given by the extracted resonance energies from the fitted line shapes for the $\alpha_0$- and $\alpha_1$-decay modes. The resonance energies corresponding to various decay modes from a resonance can provide insight into the spin and parity, particularly when only a single $l$ value of decay is possible. For a $J^\pi = 0^+$ resonance in $^{16}$O, an $\alpha$ particle emitted through either $\alpha_0$ decay or $\alpha_1$ decay carries exactly $l = 0\hbar$ or $2\hbar$ units of angular momentum, respectively. If the $\alpha_0$- and $\alpha_1$-decay modes observed at $E_x \approx 15$ MeV are from the same $J^\pi = 0^+$ resonance in $^{16}$O, both the greater center-of-mass energy and the lack of a centrifugal potential barrier for $\alpha_0$ decay suggest that the extracted resonance energy of the $\alpha_0$-decay line shape should be lower than that of the $\alpha_1$ decay. From this work, the $\alpha_0$-decay mode observed at $E_x = 15.090(7)$ MeV is 44(3) keV higher in excitation energy than that of the $\alpha_1$-decay mode. It is therefore incompatible for the $\alpha_0$- and $\alpha_1$-decay modes to both originate from a single $J^\pi = 0^+$ resonance. In principle, this shift in resonance energies could be explained by the existence of either a single $J^\pi = 2^+$ resonance or a single $J^\pi = 3^-$ resonance: the minimal orbital angular momenta for $\alpha_0$ and $\alpha_1$ decay are $l = 2\hbar$ or $0\hbar$, respectively, for a $J^\pi = 2^+$ resonance and $l = 3\hbar$ or $1\hbar$, respectively, for a $J^\pi = 3^-$ resonance. Assuming the $m$-state population ratios calculated with a direct single-step reaction mechanism are correct, the calculated angular correlations of $\alpha_0$ decay from both a $J^\pi = 2^+$ and a $J^\pi = 3^-$ resonance do not agree well with the data displayed in Fig. 3(e).

Finally, we note that the presence of a previously unidentified resonance at $E_x \approx 15$ MeV could explain why the extracted total width of the unresolved $J^\pi = 2^+$ resonance at $E_x = 14.930(8)$ MeV, extracted from the inclusive data to be 101(3) keV, is inconsistent with the $p_0$-extracted width and literature value of 40(1) and 54(5) keV, respectively. The observation of a smooth and featureless instrumental background spectrum (iii) in Fig. 1(c) ensures that this disparity of widths is not caused by experimental artifacts. Similarly, the inclusive excitation energy spectrum from the $^{12}$C target, displayed as spectrum (iv) in Fig. 1(c), shows that the $^{12}$C contribution at $E_x \approx 15$ MeV is negligible. Given the $\alpha$-separation energies for $^6$Li and $^7$Li of $E_{\rm sep} = 1.47$ and 2.47 MeV, respectively, the contributions of the lithium resonances to the focal plane spectra collectively form a slowly varying continuum, shown as the orange-filled line shape in Figs. 1(a) and 1(b). Furthermore, the presence of a contaminant nucleus which decays through charged-particle emission would be kinematically identified within the coincident matrix of silicon energy versus excitation energy, displayed in Fig. 1(d).

Itoh *et al.* studied the $^{16}$O($\alpha$,$\alpha'$) reaction at $\theta_{\rm lab} = 0^\circ$ and $\theta_{\rm lab} = 4^\circ$, with an incident energy of $E_{\rm lab} = 386$ MeV [28]. A multipole decomposition was performed on the differential cross section of the resonance within the excitation energy interval: 15.00 MeV $< E_x <$ 15.25 MeV. While the decomposition indicated the presence of a $0^+$ resonance, the differential cross section is qualitatively different from that of the $0^+$ resonance observed at 12.00 MeV $< E_x <$ 12.25 MeV. This is reflected by the larger fitted contribution of $L \geqslant 1$ angular momentum transfer reactions. Their work is therefore consistent with the existence of a previously unresolved resonance at $E_x \approx 15$ MeV that does not exhibit a $0^+$ nature.

By studying the $^{16}$O($\alpha$,$\alpha'$) reaction at $\theta_{\rm lab} = 0^\circ$ with an incident energy of $E_{\rm lab} = 200$ MeV, low-spin states in $^{16}$O were strongly excited. The angular correlations observed with the CAKE array suggest the existence of a previously unresolved resonance at $E_x \approx 15$ MeV with nonzero spin. This is supported by the shift in resonance energies between the $\alpha_0$- and $\alpha_1$-decay modes (see Fig. 2). The existence of a previously unresolved resonance may explain the disparity between the theoretical and experimentally observed widths of 34 and 166(30) keV, respectively. A narrower and therefore longer-lived $0_6^+$ resonance located above the 4-$\alpha$-particle breakup threshold ($S_{4\alpha} = 14.437$ MeV) could be considered a better candidate for a Hoyle-like state in $^{16}$O.

This work was supported by the South Africa National Research Foundation and, in particular, through NEP Grant No. 86052. R.N. acknowledges financial support from the NRF through Grant No. 85509.

[1] K. Ikeda, H. Horiuchi, and S. Saito, Prog. Theor. Phys. Suppl. **68**, 1 (1980).

[2] P. Schuck, Y. Funaki, H. Horiuchi, G. Röpke, A. Tohsaki, and T. Yamada, J. Phys.: Conf. Ser. **413**, 012009 (2013).

[3] J. A. Maruhn, M. Kimura, S. Schramm, P.-G. Reinhard, H. Horiuchi, and A. Tohsaki, Phys. Rev. C **74**, 044311 (2006).

[4] P. Chevallier, F. Scheibling, G. Goldring, I. Plesser, and M. W. Sachs, Phys. Rev. **160**, 827 (1967).

[5] T. Wakasa, E. Ihara, K. Fujita, Y. Funaki, K. Hatanaka, H. Horiuchi, M. Itoh, and J. Kamiya, Phys. Lett. B **653**, 173 (2007).

[6] Y. Funaki, H. Horiuchi, G. Röpke, P. Schuck, A. Tohsaki, and T. Yamada, Nucl. Phys. News **17**, 11 (2007).

[7] Y. Funaki, T. Yamada, H. Horiuchi, G. Röpke, P. Schuck, and A. Tohsaki, Phys. Rev. Lett. **101**, 082502 (2008).

[8] N. N. D. Center, *Nuclear Science References* (version from 2016), information extracted from the NSR database http://www.nndc.bnl.gov/ensdf.

[9] S. Ohkubo and Y. Hirabayashi, Phys. Lett. B **684**, 127 (2010).
[10] Y. Funaki, T. Yamada, A. Tohsaki, H. Horiuchi, G. Röpke, and P. Schuck, Phys. Rev. C **82**, 024312 (2010).
[11] Y. Funaki, H. Horiuchi, W. von Oertzen, G. Röpke, P. Schuck, A. Tohsaki, and T. Yamada, Phys. Rev. C **80**, 064326 (2009).
[12] D. Tilley, H. Weller, and C. Cheves, Nucl. Phys. A **564**, 1 (1993).
[13] T. Marvin and P. Singh, Nucl. Phys. A **180**, 282 (1972).
[14] A. Frawley, K. Bray, and T. Ophel, Nucl. Phys. A **294**, 161 (1978).
[15] O. Bilaniuk, H. Fortune, and R. Middleton, Nucl. Phys. A **305**, 63 (1978).
[16] L. L. Ames, Phys. Rev. C **25**, 729 (1982).
[17] P. J. Haigh, M. Freer, N. I. Ashwood, T. Bloxham, N. Curtis, H. G. Bohlen, T. Dorsch, Tz. Kokalova, C. Wheldon, W. N. Catford, N. P. Patterson, and J. S. Thomas, J. Phys. G: Nucl. Part. Phys. **37**, 035103 (2010).
[18] C. Wheldon, N. I. Ashwood, M. Barr, N. Curtis, M. Freer, Tz. Kokalova, J. D. Malcolm, S. J. Spencer, V. A. Ziman, T. Faestermann, R. Krücken, H.-F. Wirth, R. Hertenberger, R. Lutter, and A. Bergmaier, Phys. Rev. C **83**, 064324 (2011).
[19] R. Neveling *et al.*, Nucl. Instrum. Methods Phys. Res. A **654**, 29 (2011).
[20] P. Papka, N. Y. Kheswa, M. Msimanga, C. Pineda-Vargas, and N. S. Soić, J. Radioanal. Nucl. Chem. **305**, 713 (2015).
[21] K. C. W. Li, Masters thesis, Stellenbosch University and iThemba LABS, http://hdl.handle.net/10019.1/97982, 2015.
[22] P. Adsley, R. Neveling, P. Papka, Z. Dyers, J. W. Brümmer, C. Aa. Diget, N. J. Hubbard, K. C. W. Li, A. Long, D. J. Marin-Lambarri, L. Pellegri, V. Pesudo, L. C. Pool, F. D. Smit, and S. Triambak, J. Instrum. **12**, T02004 (2017)..
[23] R. Wells, J. Quant. Spectrosc. Radiat. Transfer **62**, 29 (1999).
[24] E. P. Wigner, Phys. Rev. **98**, 145 (1955).
[25] J. R. Comfort and M.N. Harakeh, Program CHUCK3 (1979), modified version of CHUCK by P. D. Kunz, University of Colorado (unpublished).
[26] M. N. Harakeh and L. W. Put, ANGCOR—An Angular Correlation Program, Internal Report KVI-76, 1979.
[27] S. Agostinelli, J. Allison, K. Amako, J. Apostolakis, H. Araujo, P. Arce, M. Asai, D. Axen, S. Banerjee, G. Barrand, F. Behner, L. Bellagamba, J. Boudreau, L. Broglia, A. Brunengo, H. Burkhardt, S. Chauvie, J. Chuma, R. Chytracek, G. Cooperman *et al.*, Nucl. Instrum. Methods Phys. Res. Sec. A **506**, 250 (2003).
[28] M. Itoh, H. Akimune, M. Fujiwara, U. Garg, H. Hashimoto, T. Kawabata, K. Kawase, S. Kishi, T. Murakami, K. Nakanishi, Y. Nakatsugawa, B. K. Nayak, H. Sakaguchi, S. Terashima, M. Uchida, Y. Yasuda, M. Yosoi, and J. Zenihiro, J. Phys.: Conf. Ser. **569**, 012009 (2014).